Flutter Speed Predictions for MW-Sized Wind Turbine Blades

Don W. Lobitz
Sandia National Laboratories*
Albuquerque, New Mexico 87185
dwlobit@sandia.gov

Abstract

Classical aeroelastic flutter instability historically has not been a driving issue in wind turbine design. In fact, rarely has this issue even been addressed in the past. Commensurately, of the wind turbines that have been built, rarely has classical flutter ever been observed. However, with the advent of larger turbines fitted with relatively softer blades, classical flutter may become a more important design consideration. In addition, innovative blade designs involving the use of aeroelastic tailoring, wherein the blade twists as it bends under the action of aerodynamic loads to shed load resulting from wind turbulence, may increase the blades proclivity for flutter. With these considerations in mind, it is prudent to revisit aeroelastic stability issues for a MW-sized blade with and without aeroelastic tailoring. Focusing on aeroelastic stability associated with the shed wake from an individual blade turning in still air, the frequency-domain technique developed by Theodorsen for predicting classical flutter in fixed wing aircraft has been adapted for use with a rotor blade. Results indicate that the predicted flutter speed of a MW-sized blade is slightly greater than twice the operational speed of the rotor. When a moderate amount of aeroelastic tailoring is added to the blade a modest decrease (12%) in the flutter speed is predicted. By comparison, for a smaller rotor with relatively stiff blades, the predicted flutter speed is approximately six times the operating speed. When frequently used approximations to Theodorsen's method are implemented, drastic under-predictions result, which, while conservative, may adversely impact blade design. These under-predictions are also evident when this MW-sized blade is analyzed using time-domain methods.

* Sandia is a multiprogram laboratory operated by Sandia Corporation, a Lockheed Martin Company, for the United States Department of Energy under Contract DE-AC04-94AL85000.

1 Introduction

Although classical aeroelastic flutter has generally not been a driving issue in utility scale wind turbine design, one case in which classical flutter was observed involved a vertical axis wind turbine turning in still air with variable speed capability [1,2]. The rotor was purposefully operated at ever increasing RPM until the flutter boundary was breached and dramatic classical flutter oscillations were observed. The flutter speed and associated vibratory frequency and mode shape were subsequently predicted using software developed for that purpose and, good agreement was obtained between the measured and predicted results. The flutter, incidentally, occurred at approximately twice the operating speed of the rotor.

For larger turbines fitted with relatively softer blades, classical flutter may become a more important design consideration. Innovative blade designs involving the use of aeroelastic tailoring, wherein the blade twists as it bends under the action of aerodynamic loads to shed load resulting from wind turbulence, increases the blades proclivity for flutter. As a reference point, in an earlier work for a 20 kW HAWT (Horizontal Axis Wind Turbine) rotor with stiff, aeroelastically tailored 5 m blades, Lobitz and Veers [3] predicted rotor flutter speeds that were several times the operating speed, rendering flutter a moot issue. With the prospect of encroaching stability boundaries associated with state-of-the-art rotors, it is prudent to investigate aeroelastic stability issues for MW-sized blades, and the adequacy of the approximations embodied in dynamic aeroelastic analysis design tools that have been used in the past in conjunction with smaller, stiffer blade designs where stability boundaries are remote relative to the rotor operational speeds.

The analysis of classical flutter in wind turbines necessitates the use of unsteady aerodynamics.

As pointed out by Leishman [4], for horizontal axis wind turbines there are two interconnected sources of unsteady aerodynamics. The first is a result of the trailing wake of the rotor and is addressed by investigating the interactions between the rotor motion and the inflow. The second, which will be the focus of this paper, is due to the shed wake of the individual blades and can be addressed using techniques developed for analyzing flutter in fixed-wing aircraft. To simplify the analysis for this latter source, the rotor is assumed to be turning in still air, and, thus, for no inflow, unsteady aerodynamics caused by the trailing wake can be neglected. Consequently, the aerodynamics for a single blade is similar to that of a fixed wing with a free stream velocity that varies linearly from the root to the tip, assuming that the shed wake of the preceding blade dies out sufficiently fast so that the oncoming blade will encounter essentially still air. This assumption did not seem to degrade the predictions associated with the vertical axis wind turbine mentioned above [1,2]. The blade also differs from the wing structurally in that it is centrifugally stiffened and rotating coordinate system effects are included in the equations of motion (i.e. Coriolis and centrifugal softening terms).

As a further simplification, the single blade is attached to a fixed hub that can only rotate. Hansen [5] asserts that a single blade analysis to determine aeroelastic stability is unconservative and that when the complete turbine is analyzed flutter speeds are significantly lower. However, his analysis deals only with unsteady aerodynamics associated with the interaction between the inflow and the rotor, and his claim may not be true for the unsteady aerodynamics associated with the shed wake from the blade that will be addressed here. A complete approach would combine the unsteady aerodynamics associated with both the inflow and the shed wake from the blades using a complete wind turbine model. However, the simple aeroelastic stability analysis presented here can still serve as a sanity check for use during the blade design process.

The technique modified for the aeroelastic stability analysis of a HAWT blade was developed by Theodorsen[6] and has been reproduced in several aeroelasticity textbooks [7,8]. Theodorsen's solution is couched in the frequency domain and contains both circulatory and noncirculatory aerodynamic terms. These terms are linear functions of the blade twist and its first and second time derivatives, and the first and second time derivatives of the blade plunging motion (flapping motion perpendicular to the free stream). Moreover, the circulatory terms are multiplied by a complex-valued function (the Theodorsen Function) which depends on the reduced frequency and hence, the frequency of the flutter oscillation. The presence of this function necessitates an iterative solution procedure since the flutter oscillation frequency is not known a priori.

Theodorsen's technique described above has been modified over the years in a variety of ways to simplify the solution procedure. One modification entails replacing the Theodorsen function with a unit value thereby reducing the unsteady aerodynamic theory to a quasi-steady one and eliminating the need for iteration. Other modifications involve removing terms (such as the terms that contain second derivatives in time) from the equations. To investigate the ramifications of these simplifications, aeroelastic stability predictions for a MW-sized aeroelastically tailored blade design have been made using modifications of the technique in addition to those made employing the unadulterated equations.

Computations using the time-domain ADAMS/AERODYN [9,10] software, which contains options for both the quasi-steady and unsteady aeroload computation, are made here to corroborate the frequency-domain results, and to discover possible inadequacies in simulating larger more flexible and possibly twist/coupled rotors using computational tools that rely on quasi-steady aeroload computation.

The remaining sections of the paper include a description of the analysis technique used for aeroelastic stability predictions, classical flutter speed results for the MW-sized blade model (with and without aeroelastic tailoring), and a summary with conclusions.

2 Analysis technique

As discussed above, unsteady aerodynamics is required for classical aeroelastic flutter prediction. Focusing on aeroelastic stability associated with the shed wake from an individual HAWT blade, the technique developed by Theodorsen [6,7,8] for fixed wing aircraft has

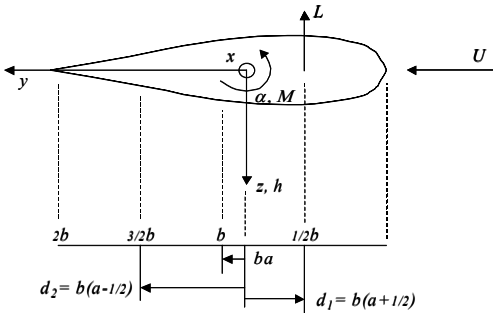

Figure 1. Blade cross section schematic.

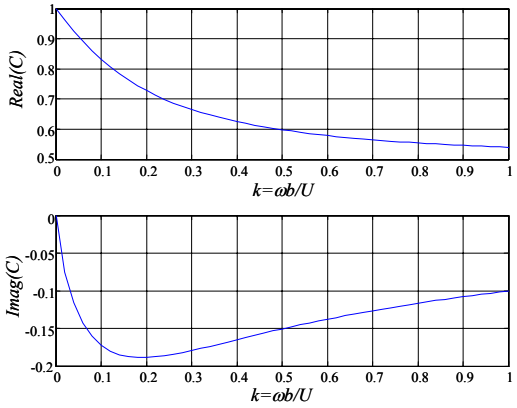

Figure 2. The Theodorsen function.

$$L = 2\pi\rho U^2 b\left\{\frac{i\omega C(k)}{U}h_0 + C(k)\alpha_0 + \left[1 + C(k)(1-2a)\right]\frac{i\omega b}{2U}\alpha_0 - \frac{\omega^2 b}{2U^2}h_0 + \frac{\omega^2 b^2 a}{2U^2}\alpha_0\right\} \quad (1)$$

$$M = 2\pi\rho U^2 b\left\{d_1\left[\frac{i\omega C(k)}{U}h_0 + C(k)\alpha_0 + \left[1 + C(k)(1-2a)\right]\frac{i\omega b}{2U}\alpha_0\right] + d_2\frac{i\omega b}{2U}\alpha_0 - \frac{\omega^2 a b^2}{2U^2}h_0 + \left(\frac{1}{8} + a^2\right)\frac{\omega^2 b^3}{2U^2}\alpha_0\right\}$$

been adapted for use with HAWT blades. Theodorsen's technique specifically addresses classical flutter in an infinite airfoil (i.e. two dimensional) undergoing oscillatory pitching and plunging motion in an incompressible flow as shown in Figure 1. The pitching motion is represented by α, and the plunging motion, by h in the figure. L represents the lift vector positioned at the ¼ chord, M is the pitching moment about the elastic axis and U is the free stream velocity. The origin of the coordinate system is positioned along the chord line at the elastic axis.

If the blade is simultaneously pitching and plunging in an oscillatory fashion as described below,

$$h = h_0 e^{i\omega t} \qquad \alpha = \alpha_0 e^{i\omega t},$$

where h_0 and α_0 are complex constants, Theodorsen shows that the lift force, L, and the pitching moment, M, are given by equations 1, where a , b, d_1, and d_2 are as shown in Figure 1. Note that a is defined as the fraction of b (the half-chord) that the elastic axis is aft of the mid-chord. Thus in Figure 1, a is negative since the elastic axis is ahead of the mid-chord. The Theodorsen function, $C(k)$, which is a complex-valued function of the reduced frequency, $k = \omega b/U$, is given by:

$$C(k) = \frac{H_1^{(2)}(k)}{H_1^{(2)}(k) + iH_0^{(2)}(k)},$$

where H denotes the Hankel function. The real and imaginary parts of C are displayed graphically in Figure 2.

In order to incorporate equations (1) in a finite element procedure for subsequent complex eigenvalue analysis, they must be recast in a pseudo time domain form for developing contributions to the finite element mass, stiffness and damping matrices. This can be accomplished by leaving the Theodorsen function as is, but using the explicit ω's in the equations to construct time derivatives, producing the following equations (2) below.

Now, using equations (2) with the principle of virtual work, contributions to the finite element stiffness, mass and damping matrices can be developed that include the complex-valued Theodorsen Function.

$$L = 2\pi\rho U^2 b\left\{\frac{C(k)}{U}\dot{h} + C(k)\alpha + \left[1 + C(k)(1-2a)\right]\frac{b}{2U}\dot{\alpha} + \frac{b}{2U^2}\ddot{h} - \frac{b^2 a}{2U^2}\ddot{\alpha}\right\} \quad (2)$$

$$M = 2\pi\rho U^2 b\left\{d_1\left[\frac{C(k)}{U}\dot{h} + C(k)\alpha + \left[1 + C(k)(1-2a)\right]\frac{b}{2U}\dot{\alpha}\right] + d_2\frac{b}{2U}\dot{\alpha} + \frac{ab^2}{2U^2}\ddot{h} - \left(\frac{1}{8} + a^2\right)\frac{b^3}{2U^2}\ddot{\alpha}\right\}$$

However, before that is done, it is noted that the HAWT blade does not conform to an infinitely long uniform wing to which the above equations apply. Rather, such quantities as the semi-chord, b, and the free stream velocity, U, vary significantly along the span of the blade. Moreover, the lift curve slope, which in the above equations is assigned the theoretical value of 2π corresponding to a flat plate, varies with blade span. These variations can be approximated by assembling a conglomerate of uniform blades, wherein the above equations are assumed to be applicable incrementally. Specifically, the quantities mentioned above are represented by a linear variation over the length of the element and included within the integral over the element length associated with the principle of virtual work.

Simplified versions of equations (2) have been used over the years. One simplification involves eliminating all terms containing $\dot{\alpha}$, $\ddot{\alpha}$, and $\ddot{h}$ from the equations. Another replaces the Theodorsen function with a constant value of unity, which corresponds to that function being evaluated at the argument of $k = \omega b/U = 0$, transforming the unsteady aerodynamic theory to a quasi-steady theory. The ramifications of these simplifications will be explored later in the paper.

The MSC NASTRAN (www.mscsoftware.com) commercial finite element software is used for this aeroelastic stability investigation. The contributions to the stiffness mass and damping matrices discussed above are supplied to NASTRAN via a NASTRAN input option. NASTRAN can accommodate non-symmetric, complex-valued matrices as are required in this effort, and it provides a number of complex eigenvalue solvers for the stability analysis.

The blades are modeled with NASTRAN beam (CBEAM) elements, which do not have a provision for the coupling between bending and twisting that is required for aeroelastic tailoring. Consequently, additional terms are added to the stiffness matrix in the manner described in [11] to effect this coupling. Additional terms are also added to the various matrices to provide for rotating coordinate system effects (Coriolis and centrifugal softening terms) using the procedure outlined in [12].

In matrix notation, the finite element equation to be used for investigating the aeroelastic stability of the wind turbine blade is given in equation (3) below, where M is the conventional mass matrix and $K(u_0,\Omega)$ is the stiffness matrix, centrifugally stiffened commensurate with displacements, u_0, resulting from centrifugal loads corresponding to the rotor rotational speed, Ω. The displacement, u, and its time derivatives represent motion about this centrifugally loaded state. The α and h degrees of freedom are included in u. The two matrices, $C_C(\Omega)$ and $K_{cs}(\Omega)$, the Coriolis matrix and the centrifugal softening matrix respectively, are due to rotating coordinate system effects and depend upon the rotational speed. Bending/twist coupling is included through the presence of the matrix K_{tc}. The aeroelastic matrices, $M_a(\Omega)$, $C_a(\omega,\Omega)$ and $K_a(\omega,\Omega)$, all depend on Ω since the free stream velocity at any blade radius is governed by it (the rotor is assumed to be turning in still air). The aeroelastic matrices, $C_a(\omega,\Omega)$ and $K_a(\omega,\Omega)$, also depend on ω, the natural frequency of the mode shape of interest, which occurs in the argument of the Theodorsen function. Since this frequency is unknown at the onset of the computations an iterative process is required for obtaining accurate results.

The iterative procedure developed for the aeroelastic stability analysis of the rotor blade is composed of the following steps:

1. Select an Ω for investigation.
2. In a quasi-static NASTRAN run, create $K(u_0,\Omega)$ for subsequent eigenvalue analysis.
3. Provide an initial guess for ω or update it from the prior calculation.
4. Using a NASTRAN complex eigenvalue solution procedure, compute modes, frequencies and damping coefficients.
5. Select a mode with a small or negative damping coefficient and return to step 3 with corresponding frequency update.
6. When the prior updated frequency is sufficiently close to the subsequently computed one, either suspend computations or modify Ω and return to step 1.

The end goal in this process is to identify the

$$\left[M + M_a(\Omega)\right]\{\ddot{u}\} + \left[C_C(\Omega) + C_a(\omega,\Omega)\right]\{\dot{u}\} + \left[K(u_0,\Omega) + K_{tc} + K_{cs}(\Omega) + K_a(\omega,\Omega)\right]\{u\} = 0 \qquad (3)$$

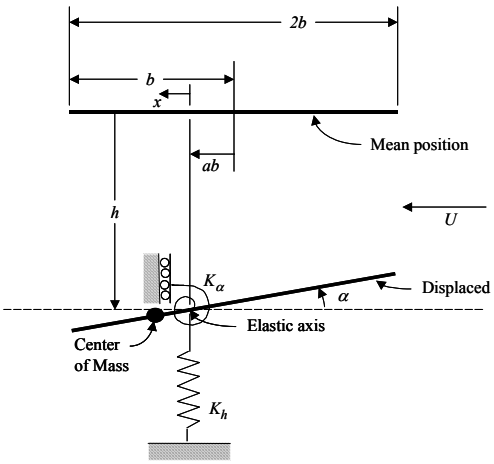

Figure 3. Schematic for the infinitely long uniform flat-plate airfoil.

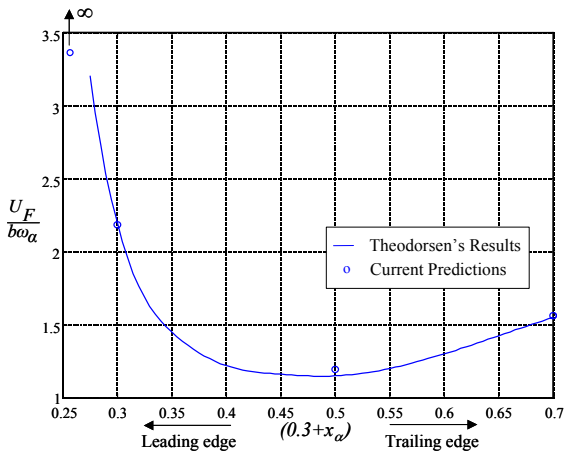

Figure 4. Flutter speed predictions for an infinitely long flat-plate airfoil with $\omega_h/\omega_\alpha = 0.707$, $r_\alpha = 0.5$, $a = -0.2$, and $m/\pi\rho_\infty b^2 = 10$.

eigenmode that exhibits a negative damping coefficient for the lowest rotor rotational speed. This speed is designated as the classical flutter speed for the blade. Usually it is associated with a mode containing a combination of twisting and flapping motion.

3 Results

Before launching into computations for a rotor blade, a few verification exercises are useful to develop confidence in this computational procedure. Solutions predicting classical flutter speeds for infinitely long uniform flat-plate airfoils in subsonic incompressible flow have been computed by Theodorsen et. al. [l3] and reproduced in [14]. A schematic of the configuration associated with these solutions is shown in Figure 3. Many of the quantities in this figure are consistent with those of Figure 1 with the exception of K_α and K_h. These represent the torsional and flapping (plunging) stiffnesses of the airfoil. Other quantities of interest in this analysis are given below:

$$x_\alpha = \frac{\int \rho x dx}{b\int \rho dx} = \frac{x_{cg}}{b}, \qquad r_\alpha^2 = \frac{\int \rho x^2 dx}{b^2 \int \rho dx} = \frac{I_\alpha}{b^2 m},$$

$$\omega_h^2 = \frac{K_h}{m}, \qquad \omega_\alpha^2 = \frac{K_\alpha}{I_\alpha},$$

where ρ is mass per unit length in the direction of the chord. As the coordinate system is positioned along the chord line at the elastic axis, the center of gravity, x_{cg}, is fore or aft of the elastic axis, depending on its sign (positive for aft). One final dimensionless group quantified in this analysis, the mass ratio, is given by $m/\pi\rho_\infty b^2$ where ρ_∞ is the free stream density.

In Figure 4, the solid curve represents Theodorsen's flutter speed (U_F) predictions for the infinitely long airfoil with the characteristics indicated in the figure caption. The curve shows how the flutter speed varies with the chordwise location of the center of mass. The circles, which correspond to predictions made using the procedure described in the preceding section, indicate that current predictions are in good agreement with Theodorsen's results. The circle to the far left associated with the infinity arrow indicates that when x_α = -0.05 the airfoil is impervious to flutter instability, consistent with the practice of mass loading the leading edge to avoid the prospect of flutter. Generally the mode shapes associated with the onset of flutter contain significant amounts of both plunging and pitching motion.

Figure 5 provides results for an infinite airfoil with cross sectional properties (see figure caption) that are more closely aligned with a conventional wind turbine blade. As before, the circles indicate that current predictions are in good agreement with Theodorsen's results. Additional results are presented at x_α = 0.1, wherein various approximations to the complete theory are made. These modifications have been implemented over the years to simplify the computation of the aerodynamic loads. The modifications investigated here involve eliminating the terms containing $\dot{\alpha}$, $\ddot{\alpha}$, and $\ddot{h}$

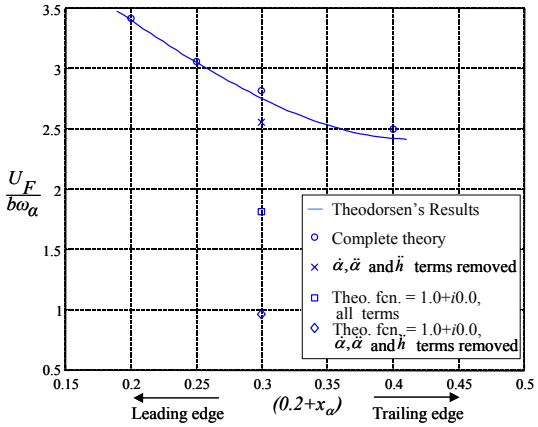

Figure 5. Flutter speed predictions for an infinitely long flat-plate airfoil with $\omega_h/\omega_\alpha = 0.133$, $r_\alpha = 0.5$, $a = -0.3$, and $m/\pi\rho_\infty b^2 = 20$.

from Equations 3 and/or approximating the Theodorsen Function with the constant value of 1.0+i0.0, which eliminates the influence of prior history on the loads. Results show that just approximating the Theodorsen Function produces a significant under-prediction of the flutter speed and, when combined with the elimination of terms, a substantial reduction occurs. While these errors are on the conservative side, they are extreme enough to adversely affect blade design.

Having developed some confidence in the computational procedure, it is applied to the large relatively soft wind turbine blade shown in the wire-frame illustration of Figure 6. This blade, termed the 'baseline' blade, was designed as part of the WindPACT Rotor Design Study [15]. Some characteristics of this blade and the associated rotor are displayed in Table 1.

Although not readily apparent from Figure 6, the blade has a modest amount of twist (11.1 deg. at the root to 0.0 deg. at the tip). The frequencies

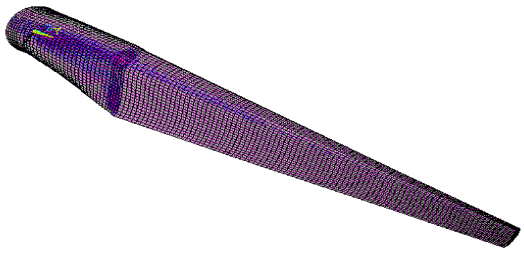

Figure 6. Wire-frame illustration of the 1.5 Mw baseline WindPACT blade.

Table 1. Characteristics of the 1.5 Mw baseline WindPACT blade and rotor.

Characteristic	**Units**	**Value**
Rated power	MW	1.5
Rotor diameter	m	70
Max rotor speed	rpm	20.5(.342 hz)
Max tip speed	m/s	75
Blade coning	deg	0
Max blade chord	m	8% of radius
Radius to blade root	m	5% of radius
Rotor solidity		0.05
Blade mass	kg	4230
Hub mass	kg	15104
Total rotor mass	kg	32016
1st flapwise frequency	hz	1.233 (1.199)
1st edgewise frequency	hz	1.861 (1.714)
2nd flapwise frequency	hz	3.650 (3.596)
1st torsional frequency	hz	9.289 (9.846)

in parentheses in this table were computed with the current computational procedure for the parked rotor configuration. They differ from the ones reported in the WindPACT study, which were computed using the ADAMS/AERODYN [10,11] software, because the two models are inherently different and only minimal efforts were made to minimize the discrepancies. In Figure 7 a planform view of the blade is presented showing the positions of the elastic axis and the axis representing the locus of the cross sectional center of gravity. As the elastic axis is forward of the mid-chord, the quantity, a, in Equations 3 is negative, and it varies along the span in a range from –0.354 to –0.284. Since in this implementation a constant value of a is required, a mid value of –0.32 has been selected.

Aeroelastic stability predictions for the rotor turning in still air were made for this baseline model and for a similar one which contained a level of flap/twist-coupling corresponding to the coupling coefficient set at 0.4 (relative to a

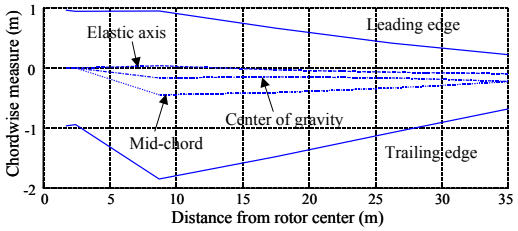

Figure 7. The 1.5 Mw baseline WindPACT blade planform showing the location of the elastic axis and the locus of the cross sectional center of gravity.

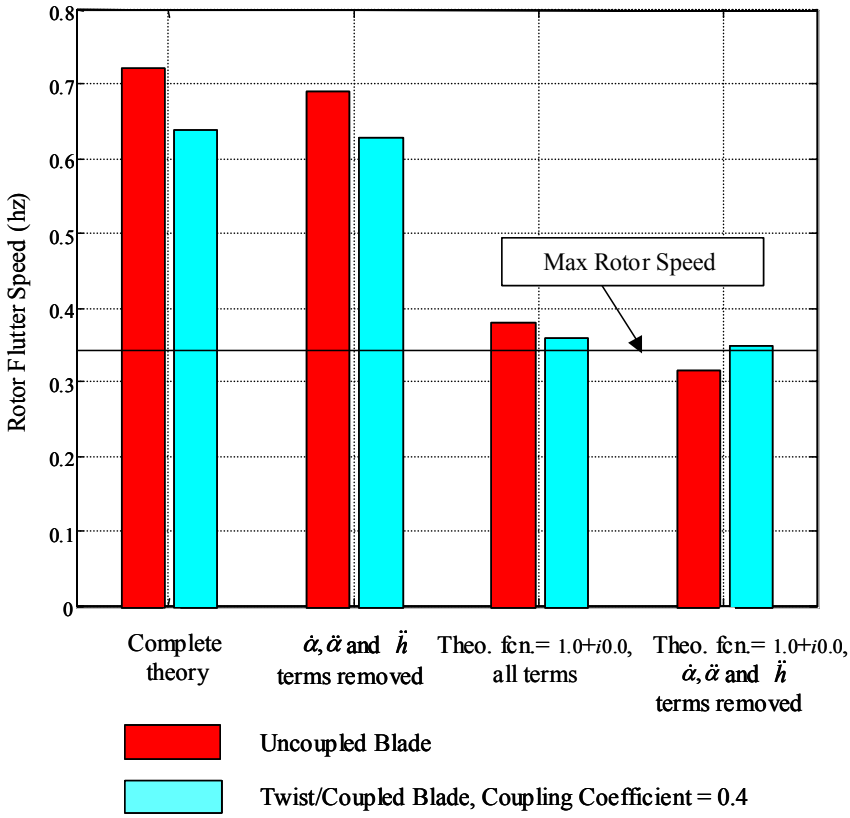

Figure 8. Flutter speed predictions for the 1.5 Mw baseline WindPACT blade for uncoupled and twist/coupled configurations. In the uncoupled configuration $\omega_h/\omega_\alpha = 0.133$, $a = -0.32$.

theoretical maximum of 1.0 based on material stability concepts [11]). Results for the predicted rotor flutter speed are reproduced in Figure 8 for both the complete theory and for various approximations to it. For the complete theory applied to the uncoupled blade, the predicted flutter speed is slightly greater than twice the operational speed of the rotor. By comparison, for the smaller rotor with relatively stiff blades examined in [3], the predicted flutter speed was approximately six times the operating speed. When a moderate amount of flap/twist-coupling is added to the WindPACT blade a modest decrease in the flutter speed is predicted. For the baseline blade the complex mode shapes associated with the onset of flutter contain significant amounts of edgewise (motion in the direction of the chord), flapping and pitching motion, as shown in Figure 9. In classical flutter, motion in the edgewise direction is generally minimal, and the large amount predicted here is thought to be due to the fact that the blade is twisted and that the frequency of the second edgewise mode (6.153 Hz) is close to the frequency of the flutter mode (6.234 Hz). In fact when flutter predictions are made for an entirely similar blade that is not twisted, edgewise motion in the associated mode is minimal.

Observing the results for the approximate theories in Figure 8, the ones that include approximating the Theodorsen Function with the constant value of 1.0+i0.0, yield relatively drastic under-predictions, with the flutter speeds dropping into the vicinity of the operating speed. The character of the damping coefficient curve as a function of rotor speed is also markedly different as shown in Figure 10. The characteristic and substantial rise in damping prior to the onset of flutter is absent when the above approximation is implemented. The decline of the natural frequency of the flutter mode is similar for full and approximate cases (see Figure 10). Approximating the Theodorsen Function with the constant value of 1.0+i0.0,

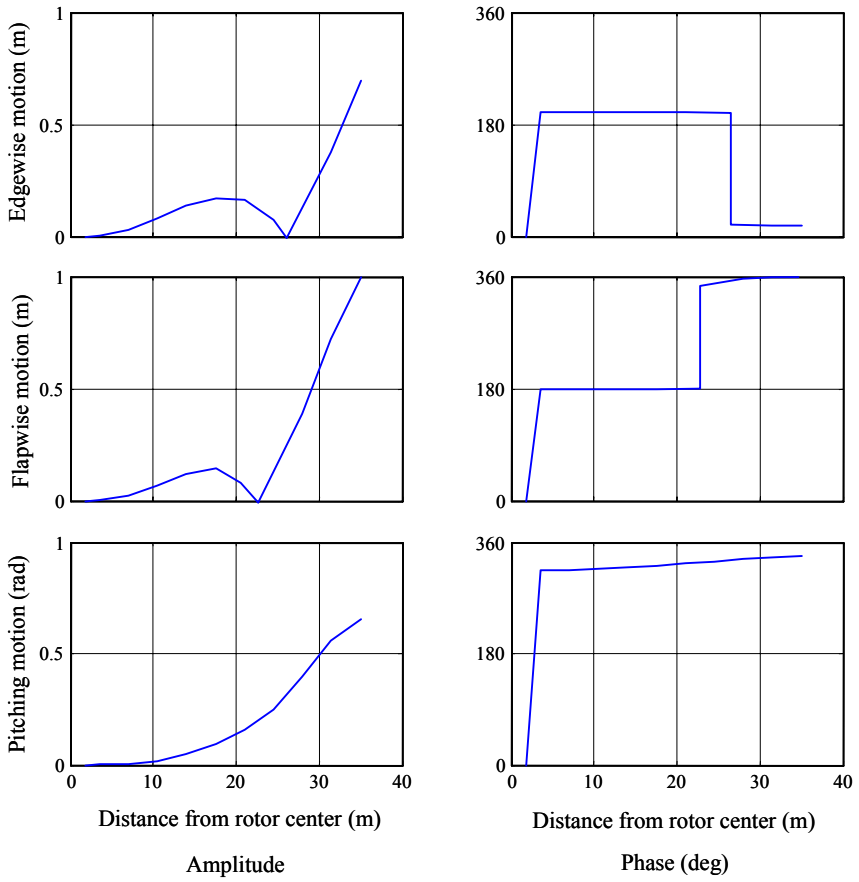

Figure 9. Mode shape at the onset of flutter for the 1.5 Mw baseline WindPACT uncoupled blade.

essentially eliminates the influence of prior history on the aerodynamic loads, reducing the unsteady aerodynamic theory to a quasi-steady one. A time domain equivalent of the Theodorsen function, as indicated by Leishman [4], is available through the use of the Wagner Function. Appropriate CFD procedures can also capture this history-dependent (unsteady) aerodynamic behavior . For transient computations that do not include this history effect, stable solutions for this particular blade may be difficult to obtain.

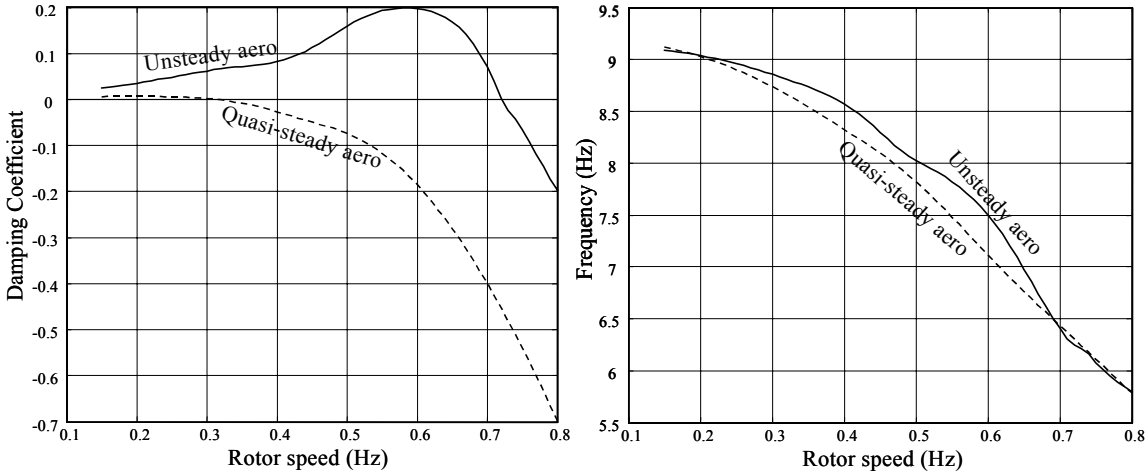

Figure 10. Damping coefficient and frequency of the flutter mode versus rotor speed for unsteady and quasi-steady aerodynamics.

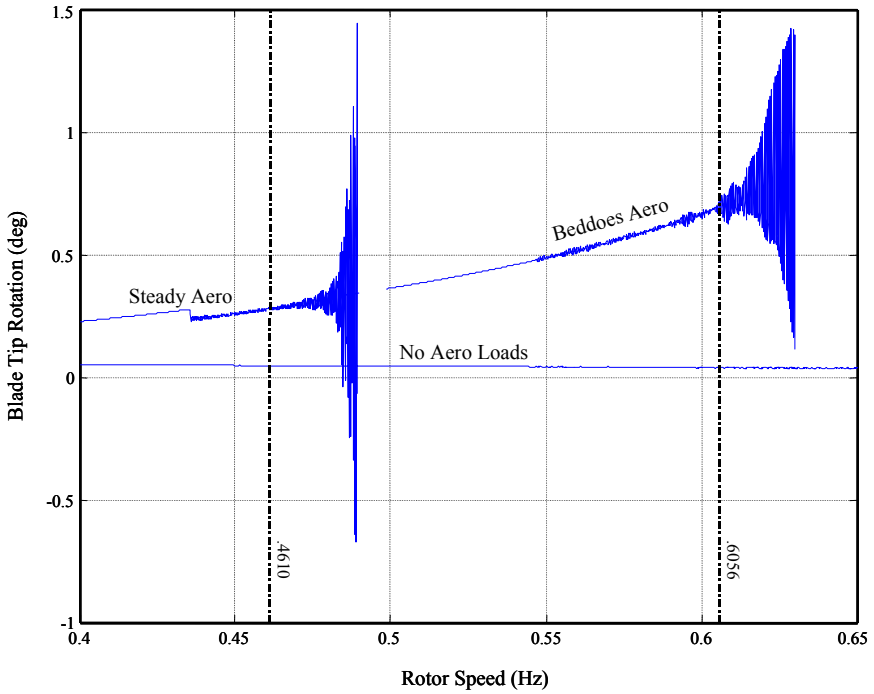

Figure 11. Quasi-steady (AERODYN "Steady" option) and unsteady (AERODYN "Beddoes" option) time domain instability predictions for the 1.5 Mw baseline WindPACT uncoupled blade.

In fact, results for the 1.5 Mw baseline WindPACT blade turning in still air, obtained using the ADAMS/AERODYN [9,10] time domain software indicate dramatic instability (characterized by tens of degrees of oscillatory pitch) at different hub rotational speeds, depending on the aerodynamic theory used. For all of these computations the blade is constrained to always be in the linear aerodynamic regime through judicious selection of the lift curves for the blade airfoils. Commensurate with the Theodorsen theory, aerodynamic drag and aerodynamic pitching moments due to airfoil section properties are assumed to be zero (an additional approximation in this analysis). In order to preserve numerical stability a small amount (0.0005) of stiffness proportional damping was included in the ADAMS model. Generally, any structural damping tends to increase flutter speeds, but the small amount included in this analysis is thought to have minimal effect.

When the "STEADY" option in AERODYN is selected, wherein the aeroloads are computed using instantaneous values of the motion (α, $\dot{h}$, etc.), i.e. quasi-steady aerodynamics, the onset of instability occurs at a rotor speed of 0.4610 Hz, as shown in Figure 11. Only the initiation of the instability is shown and not its growth to tens of degrees of oscillation. In order to trigger the instability, a force was suddenly applied at the quarter chord near the tip of the blade at a rotor speed of approximately 0.435 Hz. The torsional oscillations from this suddenly applied load tend at first to be slowly dying out but then exhibit an exponential growth pattern indicative of instability. The principal frequency of the unstable pitch oscillation is 7.02 Hz., down from the frequency of the torsional mode reported in Table 1, as is characteristic for flutter instability. When the "BEDDOES" (Beddoes-Leishman dynamic stall model [4]) option in AERODYN is selected, which utilizes the Wagner function to calculate aeroloads that depend on the history of the motion in addition to instantaneous values, i.e. unsteady aerodynamics, the onset of the instability occurs at a rotor speed of 0.6056 Hz, shown also in Figure 11. Again only the initial segment of the unstable behavior is displayed. No artificial trigger was required in this case as the numerical solution exhibits low-level noise beginning at a rotor speed of approximately 0.55 Hz. The principal frequency of the unstable pitch oscillation is 6.67 Hz., also down from the frequency of the torsional mode reported in Table 1. When the aeroloads are turned off the solution displayed in Figure 11 is entirely stable

over the rotor speed range. Evidence of numerical noise noted above, although much diminished, is apparent in this case also, beginning near the same rotor speed.

The ADAMS/AERODYN instability points are in qualitative agreement with those obtained using the Theodorsen theory for the uncoupled blade, as shown in Figure 8. For the "STEADY" aeroload option a moderately greater rotor flutter speed is predicted relative to the Theodorsen results, and, for the "BEDDOES", somewhat less than the Theodorsen predictions. Some discrepancy is expected as the frequency domain approach utilizes finite element theory and the time domain approach relies on a lumped spring/mass theory. In fact evidence exists in Table 1 of discrepancies between computed natural frequencies for the two computational methods, that could provide a plausible explanation for the discrepancies in the rotor flutter speeds noted here.

4 Summary and Conclusions

With the advent of larger turbines fitted with relatively softer blades, classical flutter may become a more important design consideration. In addition, innovative blade designs involving the use of aeroelastic tailoring, wherein the blade twists as it bends under the action of aerodynamic loads to shed load resulting from wind turbulence, may increase the blades proclivity for flutter. With the above considerations in mind, classical flutter issues are revisited for the baseline WindPACT blade (1.5 MW rotor) turning in still air for both uncoupled and twist/coupled (coupling coefficient of 0.4) configurations. Using a frequency-domain analysis tool verified with solutions obtained in the literature for two-dimensional, uniform, flat-plate airfoils, results for the uncoupled blade indicate that the rotational speeds at the incidence of flutter are approximately twice the operational speed. In comparison, flutter speeds for smaller stiffer blades are predicted to be several times the operating speed. When twist/coupling is incorporated in the blade, a modest (12%) reduction in the flutter speed is observed.

Flutter results for simplifying approximations to the full theory show that approximating the Theodorsen Function with the constant value of $1.0+i0.0$, yields relatively drastic under-predictions, with the flutter speeds dropping into the vicinity of the operating speed. This approximation essentially eliminates the influence of prior history on the aerodynamic loads, transforming the unsteady aerodynamic theory to a quasi-steady aerodynamic theory. Corroborating time domain computations have been completed here using the ADAMS/AERODYN software. In the time domain the unsteady aerodynamics are included through the use of the Wagner function, an option that is available in this software package. Computational results for both quasi-steady and unsteady aerodynamic theories support the frequency domain results, with the flutter rotor speed from the quasi-steady theory substantially less than that from the unsteady theory. As larger more flexible and possibly twist/coupled HAWT blades tend to experience classical flutter at lower relative rotational speeds (compared to their operational speed) than their smaller stiffer counterparts of the past, theoretical approximations that remove the influence of unsteady aerodynamic effects result in computational rotor flutter speeds that can approach rotor operational speeds. While conservative for avoiding flutter, this error may adversely affect blade design, either by indicating premature flutter, or, more covertly, by significantly reducing the aerodynamic damping relied upon to mitigate blade vibration. The ability to obtain stable time-domain solutions may also be compromised.

5 Acknowledgements

The author wishes to express his appreciation to David Laino of Windward Engineering for his assistance in setting up AERODYN input files and execution procedures to obtain desired computational results from the ADAMS/AERODYN software package.

6 References

[1]. Popelka, D., *Aeroelastic Stability Analysis of a Darrieus Wind Turbine*, Sandia National Laboratories Report, SAND82-0672, February 1982.

[2]. Lobitz, D. W. and Ashwill, T. D., "Aeroelastic Effects in the Structural Dynamic Analysis of Vertical Axis Wind Turbines," Proceedings of Windpower '85,

San Francisco, CA, August 27-30, 1985; 82-88.

[3]. Lobitz. D. W. and Veers, P. S., "Aeroelastic Behavior of Twist-Coupled HAWT Blades," Proceedings of the 1998 ASME/AIAA Wind Energy Symposium, Reno, NV; 75-83.

[4]. Leishman, J. G., "Challenges in Modelling the Unsteady Aerodynamics of Wind Turbines," Wind Energy 2002, **5**: 85-132.

[5]. Hansen, M. H., "Vibrations of a Three-Bladed Wind Turbine due to Classical Flutter," Proceedings of the 2002 ASME/AIAA Wind Energy Symposium, Reno, NV; 256-266.

[6]. Theodorsen, T., *General theory of aerodynamic instability and the mechanism of flutter*, *NACA Report 496*, 1935.

[7]. Fung, Y. C., *An Introduction to the Theory of Aeroelasticity*. Dover Publications Inc.: New York, 1969; 210-216.

[8]. Dowell, E. E. (Editor), *A Modern Course in Aeroelasticity*. Kluwer Academic Publishers: Dordrecht, 1995; 217-227.

[9]. MSC.Software Corporation, ADAMS product, (www.mscsoftware.com), accessed November 18, 2003.

[10].*AeroDyn Users Guide*, Version 12.50, Windward Engineering, LC, Salt Lake City, Utah, (www.windwardengineering.com), accessed November 18, 2003.

[11].Lobitz D. W. and Veers, P.S., "Load Mitigation with Bending/Twist-Coupled Blades on Rotors Using Modern Control Strategies", Wind Energy 2003; 6:2, 105-117.

[12].Lobitz, D. W., "A NASTRAN-Based Computer Program for Structural Dynamic Analysis of Horizontal-Axis Wind Turbines," *Collected Papers on Wind Turbine Technology*, DOE/NASA/5776-2, NASA CR-195432, May 1995, 89-97.

[13].Theodorsen, T. and Garrick, I. E., *Mechanism of Flutter, a Theoretical and Experimental Investigation of the Flutter Problem*, NACA Report 685, 1940.

[14].Bisplinghoff, R. L. and Ashley, H., *Principles of Aeroelasticity*, John Wiley and Sons, Inc.: New York, 1962; 246-250.

[15].Malcolm, D. J. and Hansen, A. C., *WindPACT Rotor Turbine Design Study*, National Renewable Energy Laboratory, Report NREL/SR-500-32495, August 2002.